Materials Today Bio 20 (2023) 100659

Contents lists available at ScienceDirect

Materials Today Bio

journal homepage: www.journals.elsevier.com/materials-today-bio

Glycopolypeptide hydrogels with adjustable enzyme-triggered degradation: A novel proteoglycans analogue to repair articular-cartilage defects

Yinghan Hu [a,1], Chengqi Lyu [a,1], Lin Teng [b], Anqian Wu [a], Zeyu Zhu [a], YuShi He [c], Jiayu Lu [a,*]

[a] Department of Stomatology, Shanghai Sixth People's Hospital Affiliated to Shanghai Jiao Tong University School of Medicine, Shanghai, 200233, China
[b] Shanghai Key Laboratory of Electrical Insulation and Thermal Aging, School of Chemistry and Chemical Engineering, Shanghai Jiao Tong University, Shanghai, 200240, China
[c] Shanghai Electrochemical Energy Devices Research Center, School of Chemistry and Chemical Engineering, Shanghai Jiao Tong University, Shanghai, 200240, China

ARTICLE INFO

Keywords:
Glycopolypeptide
Hydrogels
Proteoglycans analogues
ECM
Cartilage repair
Tissue regeneration engineering

ABSTRACT

Proteoglycans (PGs), also known as a viscous lubricant, is the main component of the cartilage extracellular matrix (ECM). The loss of PGs is accompanied by the chronic degeneration of cartilage tissue, which is an irreversible degeneration process that eventually develops into osteoarthritis (OA). Unfortunately, there is still no substitute for PGs in clinical treatments. Herein, we propose a new PGs analogue. The Glycopolypeptide hydrogels in the experimental groups with different concentrations were prepared by Schiff base reaction (Gel-1, Gel-2, Gel-3, Gel-4, Gel-5 and Gel-6). They have good biocompatibility and adjustable enzyme-triggered degradability. The hydrogels have a loose and porous structure suitable for the proliferation, adhesion, and migration of chondrocytes, good anti-swelling, and reduce the reactive oxygen species (ROS) in chondrocytes. In vitro experiments confirmed that the glycopolypeptide hydrogels significantly promoted ECM deposition and up-regulated the expression of cartilage-specific genes, such as type-II collagen, aggrecan, and glycosaminoglycans (sGAG). In vivo, the New Zealand rabbit knee articular cartilage defect model was established and the hydrogels were implanted to repair it, the results showed good cartilage regeneration potential. It is worth noting that the Gel-3 group, with a pore size of 122 ± 12 μm, was particularly prominent in the above experiments, and provides a theoretical reference for the design of cartilage-tissue regeneration materials in the future.

1. Introduction

Cartilage is a thin layer of dense connective tissue covering the surface of a joint, and its absence leads to physiological-function disorders, such as joint load, lubrication, and cushioning pressure [1,2]. If the cartilage defect is not improved, it may further develop into OA. So far, no effective treatments have been explored that can be incorporated into OA treatment guidelines [3,4]. Finding a treatment that can repair cartilage defects with minimal trauma and alleviate the progression of OA [5–7] has become an urgent clinical problem.

With the vigorous development of the intersection of medicine and engineering, tissue-regeneration engineering has become an important method for researchers to explore cartilage repair [8–11]. Cartilage is a tissue composed of water, cartilage extracellular matrix and a single cell type, the chondrocytes [12–17]. PGs, also known as a lubricant, is the most important polysaccharide in cartilage's ECM [11,18]. It is composed of core protein and sGAG chain connected by one or more covalent bonds [18–20]. Studies have shown that proteoglycan degradation can be used as a pathological marker of OA lesions [21]. However, there are still no functional and therapeutic substitutes for PGs. The main problems are as follows: 1) The quality of PGs production batches is inconsistent and they are expensive to produce; 2) the biodegradability and cellular-signal transduction ability of the polymers that make up the core-protein backbone need to be improved [22].

Poly-L-lysine (PLL) is a short peptide polymerized by lysine, which is one of the essential amino acids in the human body. This cationic water-soluble polymer has good adhesion, antibacterial, and non-immunity properties [23]. Studies have shown that PLL-based peptides can not only adhere to chondrocytes, but also increase the cell-to-cell contact and communication. They also stimulate mesenchymal stem cells (MSCs) to express cartilage genes in the early cartilage-formation stage [24–26]. All the evidence shows the application prospects of PLL in cartilage-tissue

* Corresponding author.
E-mail address: angelinelu@sjtu.edu.cn (J. Lu).
[1] These authors contributed equally to this work.

https://doi.org/10.1016/j.mtbio.2023.100659
Received 17 January 2023; Received in revised form 28 April 2023; Accepted 4 May 2023
Available online 11 May 2023

regeneration engineering. Unfortunately, the positive charge of PLL makes it cytotoxic to a certain extent, and PLL-based peptide hydrogels have weak stability and mechanical properties [27].

Dextran (Dex) is a type of polymer-compound glucan with a molecular weight of 440 MDa. It has good biocompatibility, high natural abundance, high hydrophilicity, and high chemical-functional modification by changing the position, length and molecular weight of branch chains. Dex oxidizes to oxidized dextran (OD) with aldehyde groups, which can react with the Schiff base in the amino group [28]. Studies have shown that the hydrogels with OD can react with amino groups on the cartilage surface to provide good tissue adhesion. They can also improve the hydrogels' mechanical strength, high porosity, and biocompatibility, which is beneficial to the proliferation of rabbit chondrocytes and chondrogenesis in vitro [29,30].

In this study, based on a simulation of the PGs structure, PLL - glucose lactone (glu) (Pg) as a core protein and OD as polysaccharide were proposed. The two were reversibly combined using a Schiff-base reaction to form a new PGs analogue, glycopolypeptide POD hydrogels. Our goal was to adjust the biocompatibility and biodegradability of the hydrogels through a series of combinations of different Pg and OD concentrations using a simple, convenient, and low-cost preparation method. Then, the hydrogels were characterized, and combined with the experimental data, three groups of concentrations were selected for in-depth biological experiments, including Gel-1, Gel-2 and Gel-3. Finally, Gel-3 as the optimal combination of Pg and OD was selected, which had good biocompatibility and good biodegradability matched with cartilage regeneration. In addition, it can adhere to chondrocytes to promote chondrocyte proliferation, differentiation and migration to the defect area to repair cartilage tissue defects.

2. Methods

2.1. Materials

Gluon-Delta-Lactone (GDL) was purchased from Sigma (USA). PLL was obtained from the School of Chemical Engineering, Shanghai Jiaotong University (China). Dextran and sodium periodate were obtained from Macklin (China). Dimethyl sulfoxide (DMSO) and triethylamine (TEA) were purchased from Titan (China). The cell-counting kit 8 (CCK-8) reagent and reactive oxygen species (ROS) assay kit was purchased from Beyotime (China). A LIVE/DEAD cell-staining kit was purchased from Sciencell (USA). A Transwell plate was purchased from Corning (USA). Papain solutions and phalloidin-TRITC were purchased from Sigma (USA). The vinculin antibody was purchased from Abcam (USA) and the Quant-iT digestion PicoGreen kit and a TRIzol reagent were purchased from Invitrogen (USA). The HiScript III RT SuperMix for quantitative polymerase chain reaction (qPCR) (+ gDNA wiper) and ChamQ Universal SYBR qPCR Master Mix (Shanghai, China) were purchased from Vazyme (China). All chemicals were used directly without additional purification.

2.2. Synthesis of the Pg and OD

The Pg was synthesized according to the method reported in the literature [31]. In short, 1.0 g of PLL and 1.1 g of GDL were dissolved in 20 ml of DMSO. Then, 1.1 ml of TEA was added and the solution was stirred violently at 50 °C for 48 h. The reaction solution was transferred to a dialysis bag and dialyzed in deionized water for 48 h molecular-weight cutoff (MWCO = 3500). After freeze-drying, a white Pg product was obtained with an 80% yield. The Pg structure was analyzed using ^{1}H nuclear magnetic resonance spectroscopy (^{1}H NMR, Mercury Plus 400, Varian, USA) and the degree of substitution of the glu group was calculated.

The OD was prepared using the reference method and modified slightly. The typical method is as follows: 1.5 g of Dex was dissolved in 5 ml of distilled water, and 1.0 g of sodium periodate was added and stirred at room temperature for 24 h. The reaction product was transferred into a dialysis bag and dialyzed in deionized water for 48 h (MWCO = 3500). After freeze-drying, a white OD product was obtained with an 80% yield. The OD structure was analyzed using ^{1}H NMR and the degree of oxidation of OD was calculated.

2.3. Preparation of glycopolypeptide hydrogels

The glycopolypeptide POD hydrogels were prepared by blending Pg and OD solutions. In short, different concentrations of Pg (4% and 5%) and OD (6%, 7% and 8%) solutions were prepared, and the two solutions were mixed at the same volume and reacted for 5 min in water bath at 37 °C. Finally, different proportions of glycopolypeptide POD hydrogels were obtained (Table 1). The gel formation was detected using a vial-inversion method.

2.4. Cell culture

All animal experiments were performed in accordance with the National Institutes of Health Guide for the Care and Use of Laboratory Animals and were approved by the Shanghai Jiao Tong University Affiliated Sixth People's Hospital (DWSY2022-0038).

Chondrocytes were obtained from articular cartilage of the knee joint of four-week-old male Sprague Dawley (SD) rats. In short, the cartilage tissues of the SD rats were aseptically collected, as much as possible was cut off, and transferred to 10-ml solutions containing 1% antibiotic–antifungal solution and 0.25% type-II collagenase for digestion. After incubating for 3 h with 5% CO_2 at 37 °C, the supernatant of the digestive juice was centrifuged at 1000 rpm for 3 min and the precipitation was collected. Then, Dulbecco's Modified Eagle Medium (DMEM, Gibco-Invitrogen, USA), containing 1% antibiotic–antifungal solution and 10% fetal bovine serum (FBS), was used to re-suspend the precipitation. The cell suspension was inoculated into a 6 cm cell-culture dish for monolayer amplification. The culture medium was changed every two days.

When the cells reached an 80% confluence, they were passed to the third generation (P3) and applied in subsequent experiments. For in vitro experiments, the treatment groups were treated with the hydrogels, while the control group only used complete medium.

2.5. In vitro cytocompatibility

The cytocompatibility of the hydrogels was tested by seeding the suspension of chondrocytes on the hydrogels and incubating for 24 h. The cells were treated using the LIVE/DEAD cell-staining kit and observed with a confocal microscope (DMI6000B, Leica, Germany). The data are expressed as the mean ± standard deviation of three repetitions.

The effect of the glycopolypeptide POD hydrogels on the chondrocyte proliferation was determined using a CCK-8 assay. In short, 100 μl of glycopolypeptide POD hydrogels were prepared at the bottom of 96-well plates and irradiated with ultraviolet (UV) light for 1 h. Cells were seeded on the surface of the hydrogels (1×10^5 cells/well), and treated with the CCK-8 reagent (10 μl/well) after incubating for 24 and 48 h respectively. The optical-density value was measured at 450 nm using an enzyme-labeling instrument (iMark, Bio-Rad, USA). All samples were measured

Table 1
Preparation of glycopolypeptide POD hydrogels.

Group	Pg concentration % (w/v)	OD concentration % (w/v)
Gel-1	4%	6%
Gel-2	4%	7%
Gel-3	4%	8%
Gel-4	5%	6%
Gel-5	5%	7%
Gel-6	5%	8%

in quintuplicate. The data are expressed as the mean ± standard deviation of three repetitions.

2.6. Biocompatibility in vivo

A full-layer skin model of the SD rats (male, 200 g–250 g) was used to evaluate the biocompatibility of the glycosylated peptide POD hydrogels in vivo. Before the operation, different proportions of samples (Gel-1, Gel-2, and Gel-3) were prepared and irradiated with UV light for 1 h. After anesthetizing the rats, a 1 cm of incision blind pouch was made in the back of the rats, and the sample was added. The skin tissue of the operation area was taken at different time points (7, 14 and 28 days after the operation). The tissue was fixed with 4% paraformaldehyde (PFA) and embedded in paraffin and sectioned serially at 5 μm. These slides were subjected to hematoxylin and eosin (H&E) staining for routine analysis, and then observed under a light microscope (n = 3).

2.7. Cell migration

The Transwell experiment was conducted to evaluate the effect of the hydrogels on chondrocyte migration. In general, 100 μl of the hydrogels were prepared and irradiated with UV light for 1 h, then placed in the lower chamber of a Transwell plate (8 μm pore diameter, Corning, USA) and immersed in a 400 μl medium. Then, 200 μl with 1×10^5 cells/ml were planted in the 24-well upper cavity.

After incubating for 48 h, the cells on the upper surface of the chamber of the Transwell were gently wiped with filter paper. The cells on the lower surface of the chamber were fixed with 4% PFA for 20 min and stained with 0.5% crystal violet for 10 min and washed three times with PBS. Finally, in each filter, five visual fields were randomly selected and counted twice by two blind independent evaluators. The data are expressed as the mean ± standard deviation of three repetitions.

2.8. Intracellular ROS detection

A ROS assay kit was used for extracellular and intracellular quantification and visualization of the free radicals and ROS. Chondrocytes were co-cultured with glycopolypeptide POD hydrogels for 24 h. Then, the chondrocytes were collected and concentration was adjusted at 1×10^6 cells/ml. Dichloro-dihydro-fluorescein diacetate (DCFH-DA) was diluted 1:1000 in a serum-free medium and incubated in a cell incubator at 37 °C for 20 min. It was mixed upside down every 3–5 min so that the probe was in full contact with the cell.

The cells were washed three times with a serum-free cell-culture medium to remove the residual probes, then collected and transferred to a new 24-well plate. The fluorescence values were measured by a microplate reader (iMark, Bio-Rad, USA). The data are expressed as the mean ± standard deviation of three repetitions.

2.9. Cell adhesion

The distribution of F-actin and focal adhesion sites was observed using phalloidin-TRITC and vinculin, respectively. In short, P3-generation chondrocytes were cultured on hydrogels for 48 h, and then fixed in 4% PFA at room temperature for 20 min. They were treated with 1% TritonX-100 for 20 min, incubated with 1% bovine serum albumin (BSA) at 37 °C for 1 h, then incubated in 1:300 diluted vinculin at 4 °C overnight.

The next day, the solutions were poured out and washed with phosphate-buffered saline (PBS) three times, each time for 5 h at room temperature. Then, the second antibody (mouse anti-rabbit) and phalloidin-TRITC were added and the cells were incubated in darkness for 1 h. The second antibody was poured out and the cells were washed with PBS three times for 5 min each time. The adhesion of the chondrocytes to the material was observed by inverted confocal microscope (DMI6000B, Leica, Germany) at Ex/Em = 556/574 nm. Finally, the ImageJ image-processing software was used to measure the area of F-actin and focal adhesion sites [32].

2.10. Biochemical assay

After the chondrocytes were cultured in hydrogels for 14 days, specimens were collected and washed with PBS, and digested with papain solutions (125 U/ml, Sigma) for 16 h at 57 °C. The papain digestible product was stored at −20 °C to await further analysis. The total DNA content of the digested sample was determined by the Quant-iT digestion PicoGreen kit, according to the manufacturer's instructions. The standard curve was generated using double-stranded DNA (dsDNA).

The total sulfated sGAG content of each sample was measured by spectrophotometry using 1,9-dimethylmethylene blue dye and chondroitin sulfate as standard. The standard curve was generated using bovine trachea chondroitin sulfate A (Sigma-Aldrich).

2.11. Real-time PCR

After the chondrocytes were cultured in hydrogels for 28 days, specimens were split into 1 ml of TRIzol reagent and the entire RNA was extracted according to the manufacturer's instructions. After the RNA was extracted, its concentration was measured using a NanoDrop One spectrophotometer (NanoDrop Technologies, USA). The HiScript III RT SuperMix for qPCR (+ gDNA wiper) and ChamQ Universal SYBR qPCR Master Mix kits were used for reverse transcription and quantitative PCR (RT PCR) respectively. Primer sequences are provided in Table S1.

The statistical data first normalized the gene-expression level to GAPDH, then normalized it to the sample expression level at the same time point to obtain the -ΔΔCt value. The relative gene-expression level was expressed as $2^{-\Delta\Delta Ct}$.

2.12. Cartilage-regeneration studies in vivo

Fourteen male New Zealand rabbits (3.0 ± 0.5 kg) were selected and used to evaluate the hydrogels promoting cartilage regeneration. A model of a full-thickness cartilage defect in the New Zealand rabbits was established under local anesthesia. In short, the knee joint was straightened and the lateral patella was displaced. The skin was cut to expose the trochlear surface of the knee joint, and a dental drill was used to create a full-thickness cylindrical cartilage defect (3 mm diameter, 3 mm depth) in the femoral cochlear groove. Hydrogels were used to repair the defect in the experimental group, while the cartilage defect in the control group was not treated. The animals were killed after 6 and 12 weeks for further examination.

2.13. Micro-CT

A SkyScan-1176 micro-computerized tomography (micro-CT) (Bruker Micro-CT, Belgium) system was used to scan the specimen micro-CT. NR economic software version 1.6 was used for three-dimensional reconstruction and image viewing. The cartilage was analyzed using CT-an software version 1.13.

2.14. Histological analysis

After the collected cartilage specimens were fixed in 4% PFA for 24 h, they were transferred to EDTA decalcification solution and placed at 37 °C about 2 months. The solution was updated every 3 days. Then the cartilage tissues embedded in paraffin. Next, histological sections were stained with H&E, Safranin O-Fast green, and specific primary antibodies (collagen type II, collagen type I, aggrecan, and Sox9), and the images were obtained by optical microscopy (DM6, Leica). The International Cartilage Repair Society (ICRS) scoring system was used for histological evaluation, and high scores indicating good repair [33].

2.15. Statistical analysis

All data were expressed as mean ± standard deviation. The statistically significant differences between groups were analyzed using the two-tailed *t*-test in the Graphpad Prism 9.0 statistical software. The statistical differences were significant, when *p < 0.05.

3. Results

3.1. Preparation of the glycopolypeptide POD hydrogels

In this study, the Pg was synthesized according to the preparation method mentioned in the literature [34]. Studies have shown that modifying PLL with glu can significantly improve its biocompatibility and reduce its cytotoxicity [27]. Therefore, to further tap the application potential of PLL regenerated tissue engineering, this study chose to introduce glu-modified PLL to produce Pg glycopolypeptide POD hydrogels, using a simple mixture of Pg and OD (Fig. 1a). The synthetic route of the Pg and OD is shown in Fig. 1b.

As shown in Fig. S1, the characteristic peaks of dextran appear at δ (ppm) = 4.92 (1H, -O***CH***O-) and 3.43–4.04 (5H, -CH***CHCHCHCH$_2$***O-), while OD shows three new absorption peaks at δ (ppm) = 5.70 (1H, -O***CH***CHO), 5.36–5.52 (1H, –CH$_2$***CH***CHO), and 5.19 (2H, -O***CH$_2$***CH-CHO). The weak peak of OD spectrum at 1790 cm^{-1} belonging to the stretching of the aldehyde group. The degree of oxidation of OD was calculated as the integral ratio between δ = 5.70 ppm and the sum of δ = 4.92 ppm and δ = 5.70 ppm. The results showed that the oxidation degree was 17%, indicating OD prepared successfully. The characteristic peaks of Pg assigned to the PLL skeleton were δ (ppm) = 4.33 (1H, -***CH***CH$_2$CH$_2$-), 2.97 (2H, -CH$_2$***CH$_2$***NH-), 1.79 (2H, -***CH$_2$***CH$_2$NH-), 1.65 (2H, -CH***CH$_2$***CH$_2$), and 1.41 (2H, –CHCH$_2$***CH$_2$***-), and δ (ppm) = 4.08 (1H, -***CH***(CH)$_3$CH$_2$-) and 3.60–3.85 (5H, –CH***(CH)$_3$CH$_2$***-) belonged to the proton peak of the glu group. FT-IR (KBr, cm^{-1}): 3292 (ν_{N-H}), 2943 (ν_{C-H}), 1657 (amide-I), 1548 (amide-II) (Fig. S2). The substitution degree of the glu group of Pg was calculated using the integral ratio of δ = 4.08 ppm to δ = 4.33 ppm. The results showed that the glu substitution degree was 50%, indicating Pg prepared successfully.

As shown in Fig. 1c, the mixture of Pg and OD could not form hydrogels at room temperature. However, when heated to 37 °C, the solution could convert into POD hydrogels within ~5 min by Schiff-base reaction. When tilting the vial after gelation, it can be seen that the liquid level no longer tilts with the tilt of the bottle. In addition, the extruded glycopolypeptide POD hydrogels can quickly restore its original shape, which was endowed with good self-healing and shape memory by the dynamic covalent bond (Fig. 1d).

3.2. Characterization of glycopolypeptide POD hydrogels

As chondrocytes are very sensitive to changes in the surrounding environment, the morphology, pore size, and porosity of the new PGs analogues directly affect the proliferation, migration, and growth of the chondrocytes [35]. Scanning electron microscope (SEM) results show that the hydrogels have a uniform interconnected porous structure (Fig. 2a). Among them, Gel-1, Gel-2, and Gel-3 have similar pore sizes, which are 136 ± 14 μm, 130 ± 10 μm, and 122 ± 12 μm, respectively (Fig. 2b).

The cross-linking degree of the hydrogels increases with the increase of the Pg concentration, and the pore sizes of Gel-4, Gel-5, and Gel-6 decreased significantly to 90 ± 10 μm, 87 ± 10 μm, and 87 ± 5 μm, respectively. The good porous structure gives the hydrogels a high porosity of 68%–74% (Fig. 2c).

In addition, as shown in Fig. 2d, the water content of the different hydrogels concentrations reached 93–95%, and there was no significant statistical difference ($p > 0.05$). Studies have confirmed that scaffolds with a 100–150 μm of pore diameter provide a more favorable environment for the growth and proliferation of chondrocytes [36–38]. Therefore, the hydrogels with large pore sizes, Gel-1, Gel-2, and Gel-3 were selected for further study of cartilage-tissue regeneration and repair.

The rheological behavior (Fig. S3) of the hydrogels was characterized using a rheological instrument, showing typical hydrogels characteristics. The elastic moduli of Gel-1, Gel-2, and Gel-3 were 0.6 kPa, 1.0 kPa, and 2.0 kPa respectively. With the increase in OD concentration, the mechanical properties of the hydrogels increased, owing to the enhanced intermolecular force and tighter gel network.

Furthermore, the hydrogels swelling will oppress the surrounding tissue, and may even cause it to separate from the target organ. As shown in Fig. 2e, the three groups of hydrogels showed extremely low swelling rates of only 103–110%, which confirmed that glycopolypeptide POD hydrogels have good anti-swelling properties [39].

Good biodegradability is a necessary prerequisite for biomimetic biomaterials to provide growth space for regenerated tissues [40]. As shown in Fig. 2f and g, the degradation of hydrogels in vitro showed that Gel-1, Gel-2, and Gel-3 were basically not degraded in PBS, and the mass surpluses remained 98 ± 2%, 97 ± 1%, and 99 ± 1%, respectively (28 d). It is worth noting that after 28 days of incubation with type-II collagenase

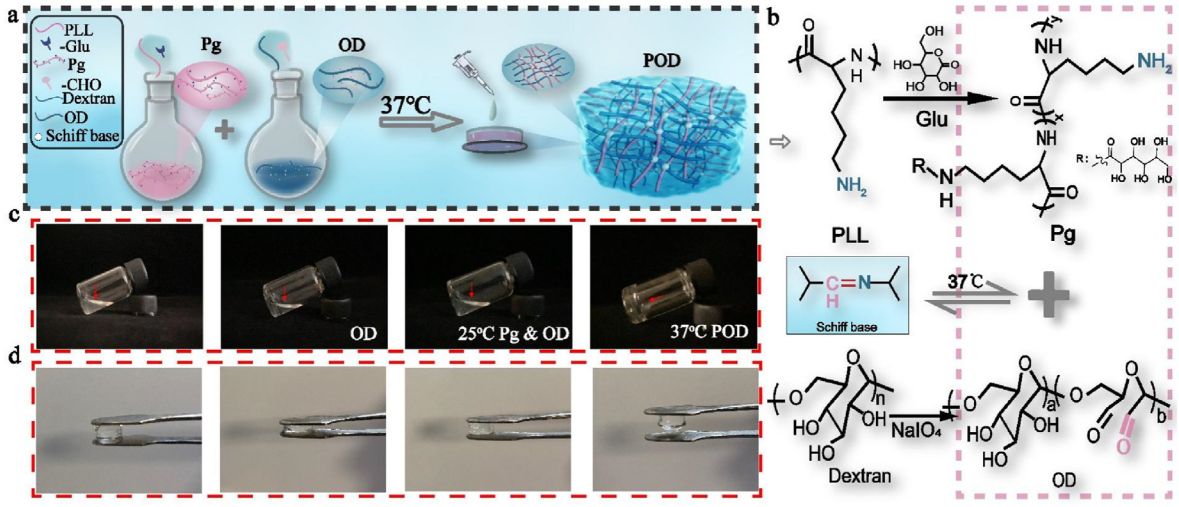

Fig. 1. Glycopolypeptide POD hydrogels. a–b) Schematic diagram of the preparation and chemical structure of the hydrogels; c) hydrogels preparation process; and d) shape memory.

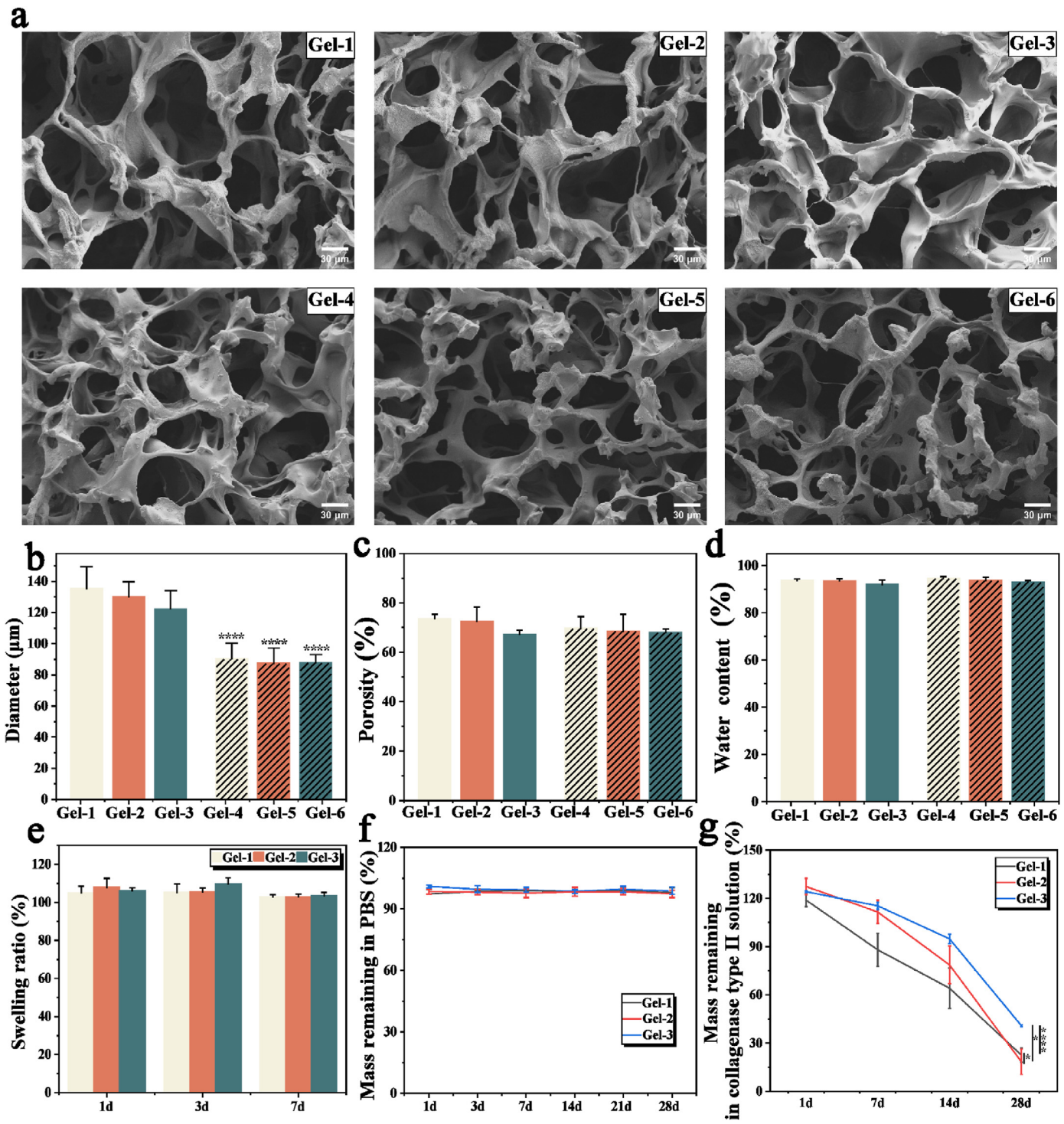

Fig. 2. Physical and chemical properties of glycopolypeptide POD hydrogels. a) SEM images, b) pore size, c) porosity, d) water content, and e) swelling properties of different concentrations of hydrogels (37 °C, PBS, 10 mM, pH 7.4). Degradability of hydrogels at 37 °C in f) PBS and g) type-II collagenase solutions (n = 5, scale = 30 μm, *P < 0.05, **P < 0.01, ***P < 0.001, ****P < 0.0001).

solutions, the quality of the Gel-1, Gel-2, and Gel-3 hydrogels decreased significantly to 23 ± 5%, 24 ± 4%, and 40 ± 1%, respectively.

The results showed that POD hydrogels have a good enzyme-mediated degradation performance, which can be regulated by changing the OD concentration to improve the spatiotemporal speed of cartilage regeneration. In summary, the anti-swelling POD hydrogels were successfully prepared. They have good biological stability and adjustable degradability, and good prospects of being used as scaffolding for cartilage regeneration.

3.3. Biocompatibility of glycopolypeptide POD hydrogels in vitro

The biocompatibility of hydrogels is an important biomaterial property. The cytotoxicity of hydrogels was evaluated by a direct-contact

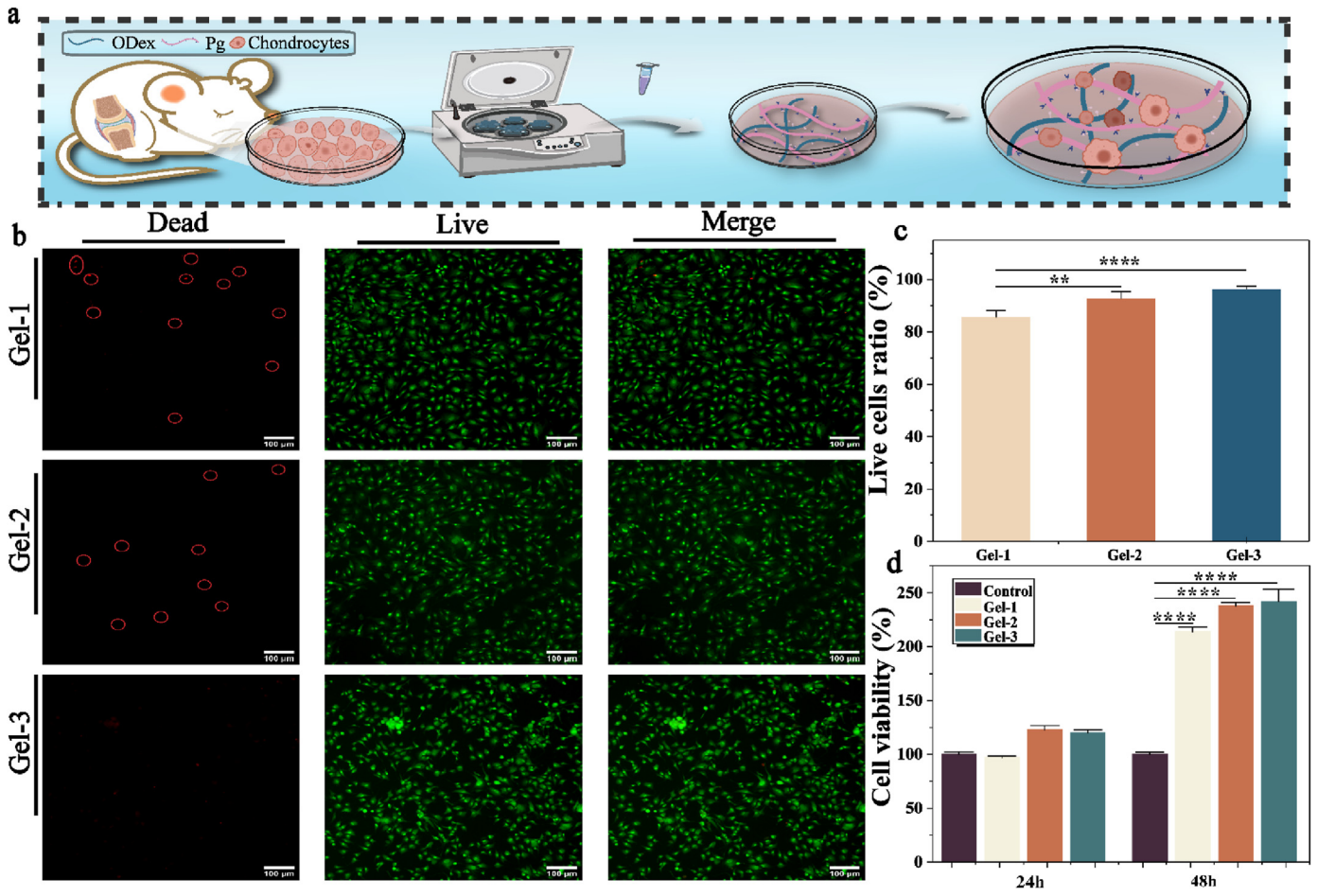

Fig. 3. Cytotoxicity of glycosylated peptide POD hydrogels in vitro. a) Cell experimental diagram of hydrogels. b) Stained picture of living (red) and dead (green) cells after 24 h of co-culture; c) proportion of living and dead cells. d) CCK-8 assay results. (n = 3, scale = 100 μm, *P < 0.05, **P < 0.01, ***P < 0.001, ****P < 0.0001).

method (Fig. 3a) [41]. As shown in Fig. 3b, the chondrocytes had a typical morphology and the number of living cells accounts for the vast majority of the visual field. The quantitative results showed that the proportion of living cells in POD hydrogels was more than 85% (Fig. 3c). It is worth noting that the proportion of living cells increased significantly from 85 ± 3% (Gel-1) to 96 ± 1% (Gel-3) with the increase of OD concentration. In summary, POD hydrogels have good cytocompatibility, and adjusting the OD concentration can significantly improve their biocompatibility.

Furthermore, the effect of hydrogels on the chondrocyte proliferation was explored using a CCK-8 assay. As can be seen in Fig. 3d, after 24 h of culture, there was no significant difference in cell viability between the hydrogels group and the control group, which once again proves the good biocompatibility of hydrogels. After 48 h of culture, the optical-density value of the hydrogels group was 2.2–2.4 times higher than that of the control group.

The above results confirmed that POD hydrogels not only have good cytocompatibility, but also significantly promote the proliferation of chondrocytes with the increase of co-culture time. It is worth noting that Gel-3 showed a maximum optical-density value (2.4), indicating that it provided a more favorable environment for chondrocyte proliferation.

The positively charged PLL easily interacts with the negative charges on the surface of the cell membrane and stimulates the growth and development of chondrocytes [23]. The adhesion of hydrogels to chondrocytes was evaluated using F-actin and vinculin fluorescence staining. As shown in Fig. 4a, the chondrocytes showed a regular morphology. The F-actin clumped around the nucleus in group Gel-1, while the diffusion in groups Gel-2 and Gel-3 was clearly seen as bundles. In contrast, with the increase of OD concentration, the adhesion plaques changed from being closely gathered around the cartilage nucleus to gradually spreading out, indicating that chondrocytes can adhere to the hydrogels.

The areas of F-actin and focal adhesion area were quantitatively analyzed using Image J2 software. As shown in Fig. 4b and c, the F-actin areas between Gel-1, Gel-2, and Gel-3 were similar, while there was significant statistical difference in the focal adhesion area between Gel-1 and the latter two groups. It is confirmed that glycopolypeptide POD hydrogels have good cell adhesion and can optimize the regulation of the OD concentration.

In addition, the Transwell experiment further showed that the hydrogels could promote chondrocyte migration. The numbers of cell migrations in Gel-1 and Gel-2 were 214–243 cell per field, respectively, while the number of cell migrations in Gel-3 increased significantly to 401 cells per field (Fig. 4d and e). The experimental results once again proved that Gel-3 provides a microenvironment to promote the growth and migration of cartilage.

Under normal physiological conditions, the growth and proliferation of chondrocytes depend on the hypoxic microenvironment in the ECM [42]; therefore, the hydrogels were required to have good antioxidant activity. The ROS production of chondrocytes was detected by a ROS kit, and the results showed that the ROS of the hydrogels group decreased significantly, as shown in Fig. 4f. In particular, the ROS content of Gel-3 decreased to 81% of that of the control group, indicating that this group had better antioxidant properties.

In vitro experiments revealed that POD hydrogels have good cytocompatibility and promote the proliferation and migration of chondrocytes. In particular, Gel-3 significantly reduces the ROS content of

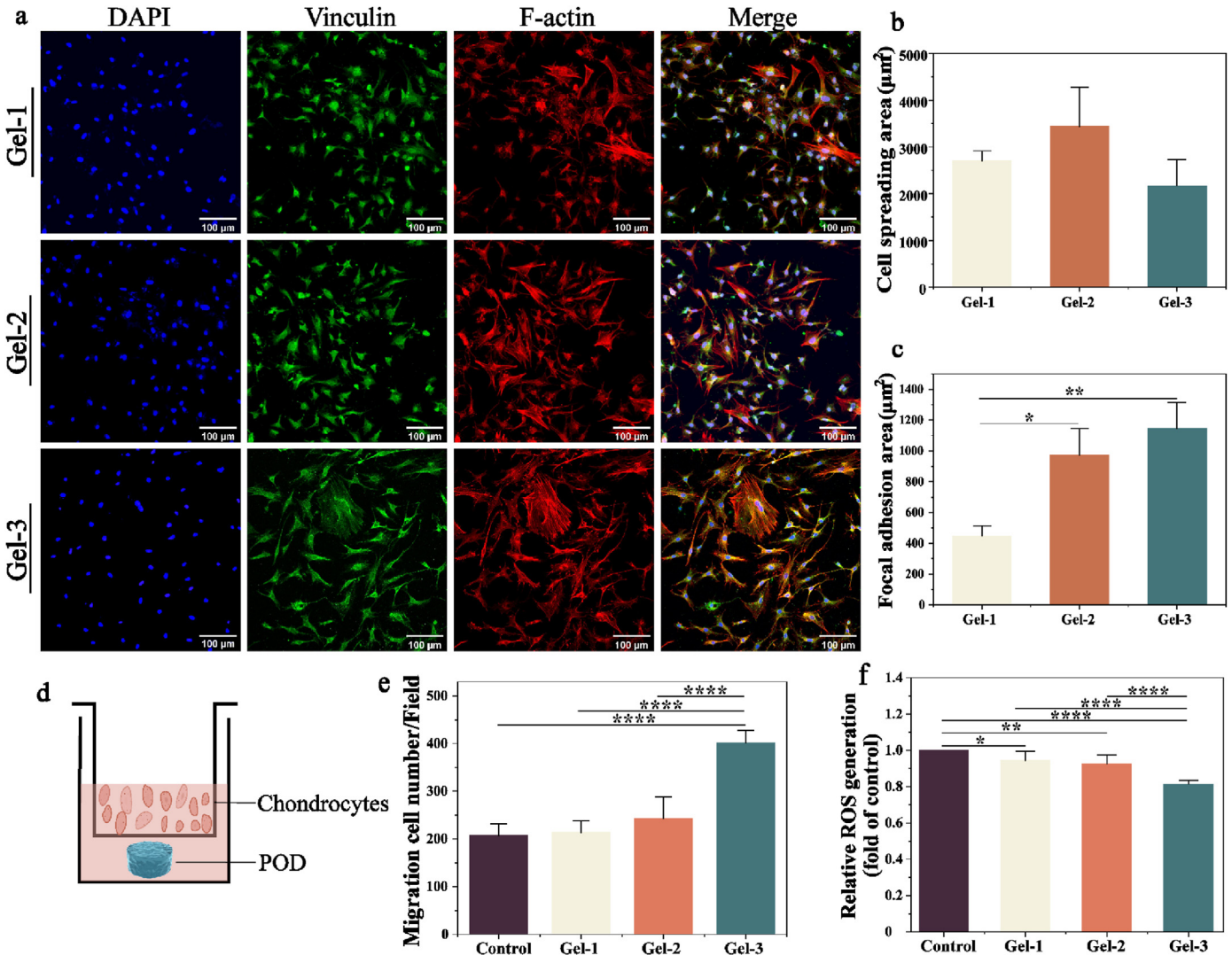

Fig. 4. Biocompatibility of glycosylated peptide POD hydrogels in vitro. a) DAPI staining of DNA (blue); the F-actin distribution was assessed using phalloidin-TRITC (red) and vinculin staining of focal adhesion (green). b) Area of F-actin and c) focal adhesion. d) Diagram of the Transwell experiment. e) Migration cell number. f) ROS production of chondrocytes. (n = 3, scale = 100 μm, *P < 0.05, **P < 0.01, ***P < 0.001, ****P < 0.0001).

chondrocytes and provides a more favorable hypoxia environment for chondrocyte regeneration. This not only alleviates the development of OA lesions, but also creates a good microenvironment for cartilage repair.

3.4. Biocompatibility of glycopolypeptide POD hydrogels in vivo

H&E staining was used to observe the inflammation of the subcutaneous skin implanted into the backs of rats at different time points, and the biocompatibility of glycopolypeptide POD hydrogels in vivo was evaluate.

As can be seen in Fig. 5, at 7 days, the implantation of different concentrations of glycopolypeptide POD hydrogels was accompanied by inflammatory-cell infiltration, as indicated by the presence of lymphocytes and neutrophils; at 14 days, the inflammatory cells decreased significantly in each group; at 28 days, not only did the inflammatory cells decrease significantly, but they were also accompanied by the emergence of neovascularization. It is worth noting that the inflammatory cells in Gel-3 decreased significantly 14 days after implantation, and only a few inflammatory cells were found 28 days after implantation.

3.5. Biochemical assay

After co-culturing glycopolypeptide POD hydrogels and chondrocytes, dsDNA, and cartilage-specific genes were quantified to evaluate the ability of glycopolypeptide POD hydrogels to promote ECM deposition, chondrocyte proliferation, and maintain the chondrocyte phenotype.

The quantitative results of dsDNA are shown in Fig. 6a. At 14 days, compared with the control group, the amount of dsDNA in Gel-2 and Gel-3 had increased significantly. The quantitative results of sGAG are shown in Fig. 6b. At 14 days, compared with the control group, the amount of sGAG in Gel-2 and Gel-3 had increased significantly. In conclusion, Gel-2 and Gel-3 promoted chondrocyte proliferation and cartilage ECM deposition.

Chondrogenesis was quantitatively evaluated using cartilage-specific genes (Fig. 6c–e). The results showed that the expressions of collagen type II, aggrecan, and sGAG genes in Gel-2 and Gel-3 were significantly higher than those in the control group. The expression of aggrecan in Gel-1 was higher than that in the control group, while the expression of sGAG

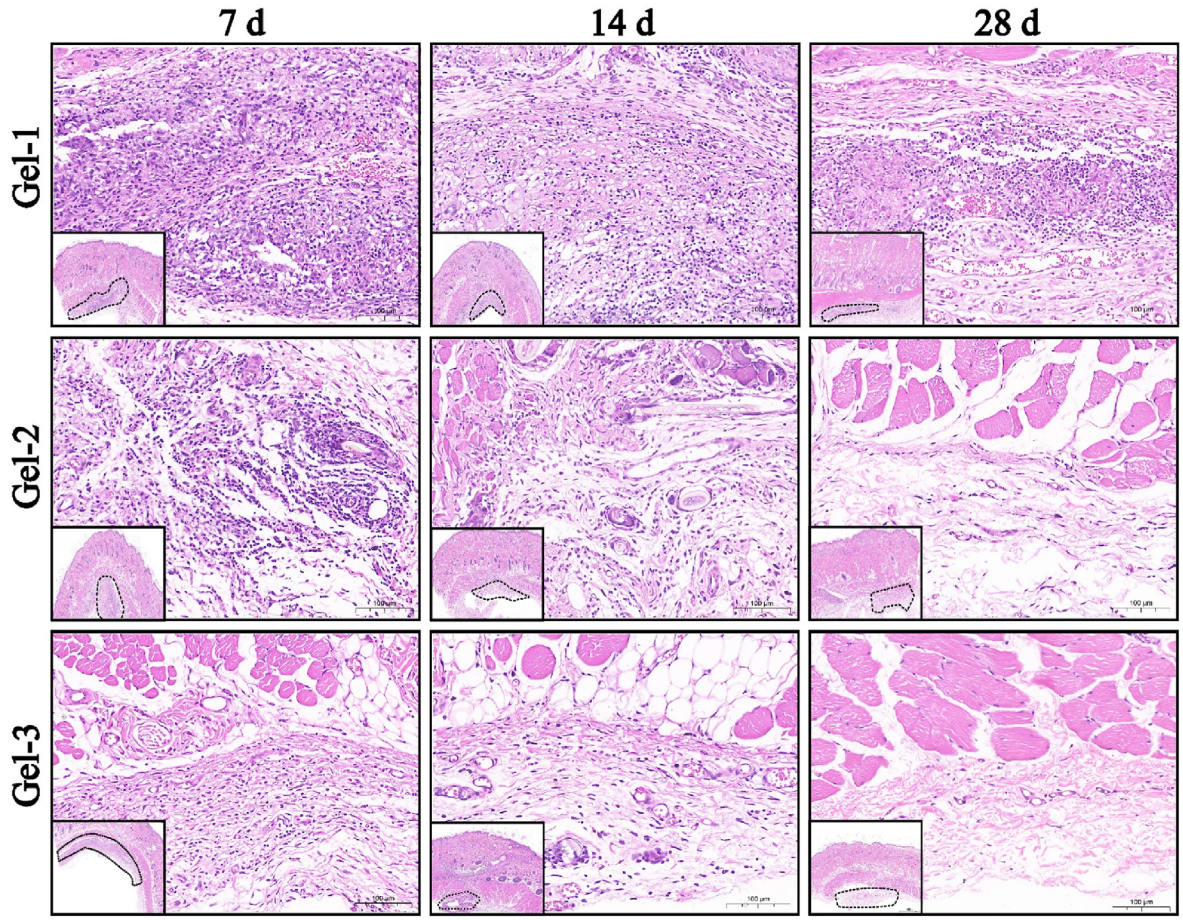

Fig. 5. In vivo biocompatibility of glycopolypeptide POD hydrogels. (n = 3, scale = 100 μm).

was significantly lower than that in the control group. Therefore, glycopolypeptide POD hydrogels promoted the expression of cartilage-specific genes in groups Gel-2 and Gel-3. The expression of collagen II and aggrecan in Gel-3 was two to three times higher than that in the control group, and Gel-3 had an excellent ability to maintain the phenotype of the chondrocytes.

3.6. *In vivo repair of cartilage with glycopolypeptide POD hydrogels*

After establishing the rabbit-knee cartilage-defect model, glycopolypeptide POD hydrogels were implanted (Fig. 7a). The results of the in vivo repair are shown in Fig. 7b. The depth and area of the cartilage defects in the hydrogels group were smaller than those of the control group. At six weeks, the hydrogels group had begun to fill the defect with obvious regenerated tissue, and a small area similar to hyaline cartilage had appeared in the Gel-2 and Gel-3; however, the defect was not completely repaired.

At 12 weeks, part of the regenerated tissue in the control group and a large area of the defect had not been restored, while the regenerated tissue in the hydrogels group was completely full of defect tissue and the surface was regular and smooth. In particular, the regenerated tissue of Gel-3 was well integrated with the surrounding tissue, and a large area of transparent tissue appeared.

Micro-CT imaging was used to evaluate the subchondral bone regeneration in postoperative cartilage defects (Fig. 7c). At 6 weeks, compared with the control group, the hydrogels group had an obvious regeneration tendency; however, the defect area was not completely repaired. At 12 weeks, part of a high-density shadow appeared in the defect area in Gel-1 and the high-density shadow in Gel-2 and Gel-3 was almost full. The boundary between most of the regenerated tissue and the surrounding tissue in Gel-3 gradually blurred.

Further data analysis (Fig. 7d–f) showed that, compared with the control group, the bone-mineral density (BMD) and bone-volume fraction (BV/TV) were up-regulated in Gel-1, Gel-2, and Gel-3 at six weeks, while the structure separation (St.Sp) was down-regulated in Gel-2 and Gel-3. At 12 weeks, the BMD and BV/TV were up-regulated and St.Sp was down-regulated in Gel-2 and Gel-3. The BMD and BV/TV values of the regenerated tissue in Gel-3 were higher than those in natural cartilage tissue, showing a good potential for regeneration.

In summary, glycopolypeptide-based POD hydrogels can effectively promote cartilage-tissue regeneration. Among them, the density of the regenerated tissue was higher and the bone trabecular space was lower in Gel-3; hence, it was the group with the best repair effect. It surpasses the natural cartilage tissue and shows good regeneration potential.

3.7. *Histological analysis*

A histological examination with H&E, Safranin-O, and immunohistochemistry (IHC) further confirmed that glycopolypeptide-based POD hydrogels repaired cartilage defects. The results are shown in Fig. 8a and b. At 6 weeks, the hydrogels group showed a clear tissue-repair tendency, with an obvious defect and less regenerated tissue in Gel-1, and large-scale repairs in Gel-2 and Gel-3 with a large number of hyaline cartilage clusters. At 12 weeks, the defect was incompletely repaired in Gel-1, and a large number of hyaline cartilage-like cells were distributed in Gel-2 and Gel-3. It is worth noting that at 12 weeks, there were more hyaline cartilage-like cells in Gel-3, and the surface of the repair area was smooth, similar to the surrounding natural tissue, and fused well. The histological

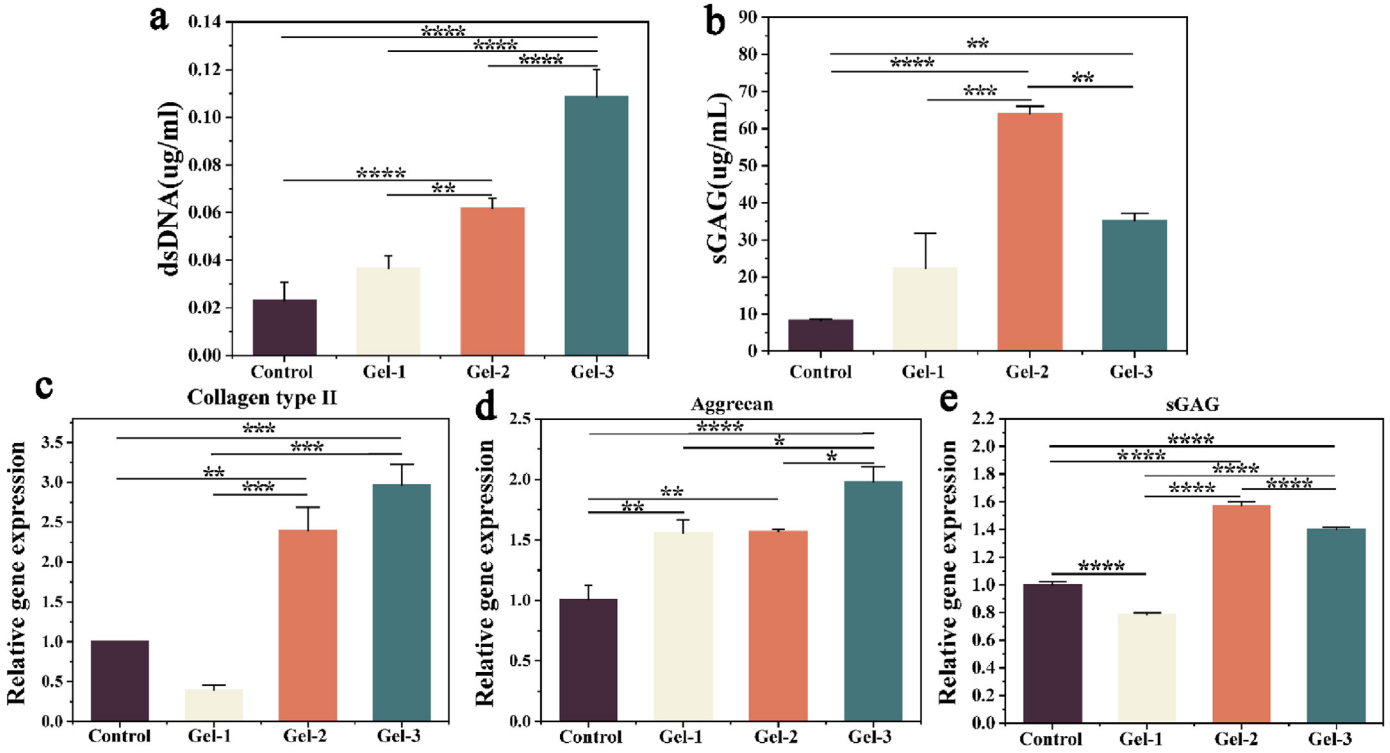

Fig. 6. Biochemical analysis. Quantification of dsDNA (a) and sGAG (b) were used to evaluate the promoting effect of glycopolypeptide POD hydrogels at different concentrations on chondrocytes. The hydrogels promote the expression of specific genes related to chondrocytes: collagen II(c), aggrecan(d), and sGAG(e). (n = 3, *P < 0.05, **P < 0.01, ***P < 0.001, ****P < 0.0001.)

score assessment showed that the Gel-3 group had the highest mean ICRS histological score (11.3–15.3), followed by the Gel-2 (9.3–11.3) and Gel-1(6.3–8.3) groups (Fig. S4). In contrast, the control group had obvious tissue defects and a small amount of thin fibrous tissue was repaired with the lowest mean ICR histological score (3.3–4.7).

The results of the IHC staining (collagen type II, aggrecan, and Sox-9) showed that there was almost no expression, with discontinuous depressions and heterogeneous tissues in the control group (Fig. 9). Type-II collagen, aggrecan, and Sox-9 were weakly positive in group Gel-1, and the defect was partially repaired. However, the expressions of type-II collagen, aggrecan, and Sox-9 were positive in Gel-2 and Gel-3, the defect was almost filled by repaired tissue, and the surface of the repaired tissue gradually became smooth. It is worth noting that the expressions of type-II collagen, aggrecan, and Sox-9 in Gel-3 were strongly positive.

In summary, it was confirmed that the hydrogels group had good cartilage-defect repair ability, and Gel-3 was the most prominent group of glycopolypeptide POD hydrogels in cartilage regeneration.

4. Discussion

Inspired by the molecular structure of natural PGs, Pg and OD were selected to prepare glycopolypeptide POD hydrogels using the Schiff-base reaction. The reaction is a reversible reaction, and the hydrolysate of the hydrogels is a polysaccharide peptide [43]. The product of the Schiff-base reaction was non-toxic, which ensured the satisfactory biocompatibility of the hydrogels. The cell proliferation, migration, and ROS detection showed that Gel-3, with the highest concentration of OD, significantly promoted the proliferation, migration, and ROS decrease of chondrocytes. This suggests that it not only has the ability to induce targeted cartilage-defect repair [44], but also has the potential to alleviate the progression of OA inflammation [45].

These were attributed to the fact that the Pg in glycopolypeptide POD hydrogels is a cationic polymer, which reacts with the negative charge on the cell-membrane surface to stimulate cell response, enhance cell viability, and promote cell proliferation [23,46], and the PLL in Pg can promote cell adhesion by up-regulating the expression of neural (N)-cadherin [47–49]. Furthermore, the appropriate concentrations of anionic OD can combine with part of the positive charge of Pg and improve the biocompatibility of the glycopolypeptide POD hydrogels, and the group Gel-3 showed the best biocompatibility in vivo and in vitro.

Chondrogenesis experiments in vitro showed that Gel-2 and Gel-3 significantly promoted the up-regulation of dsDNA, sGAG, and cartilage-related genes. Among them, the group Gel-3 significantly up-regulated collagen type II and aggrecan, and had an excellent ability to maintain the phenotype of the chondrocytes. This is because chondrocytes rely on the mechanical stimulation of the hydrogels to secrete ECM and maintain the phenotype of the chondrocytes. The increase of the cross-linking degree in Gel-3 enhanced their mechanical properties, so they showed good chondrogenesis characteristics in vitro and the ability to prevent chondrocyte dedifferentiation [50,51].

In addition, the glycopolypeptide POD hydrogels showed good tissue-regeneration potential during the repair of implanted cartilage defects in vivo, especially Gel-3. It is worth noting that the BV/TV and BMD in Gel-3 reached 72% and 73% of the natural cartilage tissue, respectively. It was followed by the appearance of a large number of hyaline cartilage-like cells and the expression of collagen type II and aggrecan. The Gel-3 had a good ability to repair cartilage defects in vivo and in vitro.

The reasons for the good cartilage-regeneration ability of the glycopolypeptide POD hydrogels in vivo and in vitro may be as follows:

1) Based on the PGs component of simulated ECM, the hydrogels aim to supplement the polysaccharides in the external chondrocyte microenvironment and maintain the integrity of the ECM tissue composition.

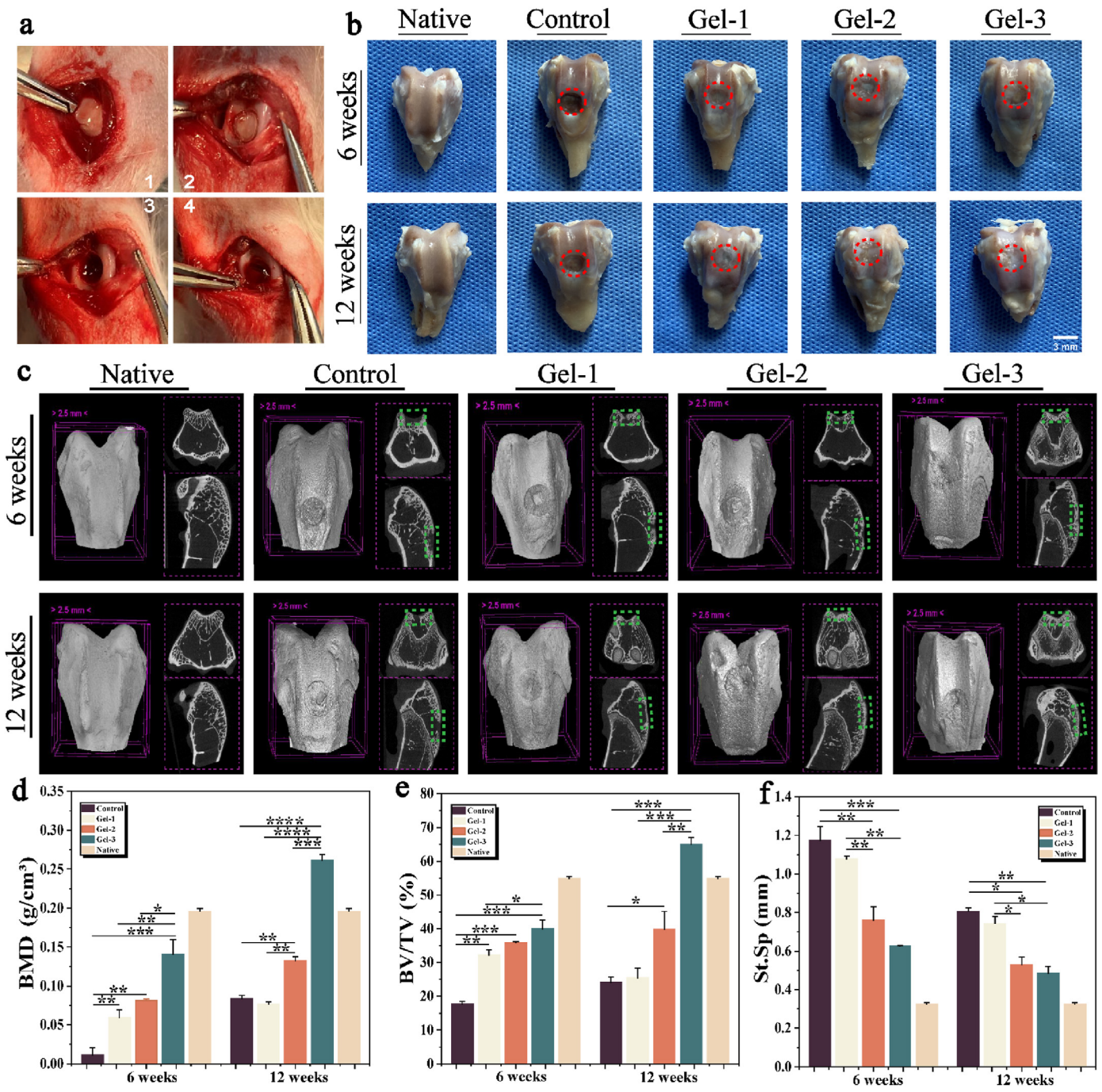

Fig. 7. Evaluation of the repair of rabbit-knee cartilage defects with glycopolypeptide POD hydrogels. a) Establishment of the rabbit-knee cartilage-defect model and implantation of hydrogels. b) Macroscopic observation of rabbit knee cartilage defect after hydrogels repair. (Red circle shows the repair area). c) Micro-CT (Green box shows the repair area). d) Analysis of related indexes of articular-cartilage defect repairs: BV/TV%, BMD, and St.Sp. (n = 3, scale = 3 mm, *P < 0.05, **P < 0.01, ***P < 0.001, ****P < 0.0001.).

2) The hydrogel's own structure restores the microenvironment of chondrocyte growth and guarantees a suitable space for chondrocyte growth, proliferation, and ECM redeposition.
3) The adjustable biodegradability of the hydrogels matches the cartilage-tissue regeneration rate, which provides support for the developing chondrocytes and degrades to make room for the growth of regenerated tissue.

Glycopolypeptide POD hydrogels can well simulate the ECM composition. sGAG, as a polysaccharide molecule on the side chain of PGs, has been widely used in clinical practice. However, sGAG is currently isolated from animal sources, and face the same batch-to-batch variation and even serious quality problems as PGs [52]. In this study, to simulate the composition and structure of PGs, the glycopolypeptide POD hydrogels were synthesized using a Schiff-base reaction, and was successfully constructed to supplement the polysaccharide components of the chondrocyte extracellular microenvironment. As a polymer network, hydrogels exhibit high water content, permeability, reasonable pore size, and porosity, which contribute to the exchange of metabolites, gases, and nutrients with the extracellular environment; hence, it is a popular choice

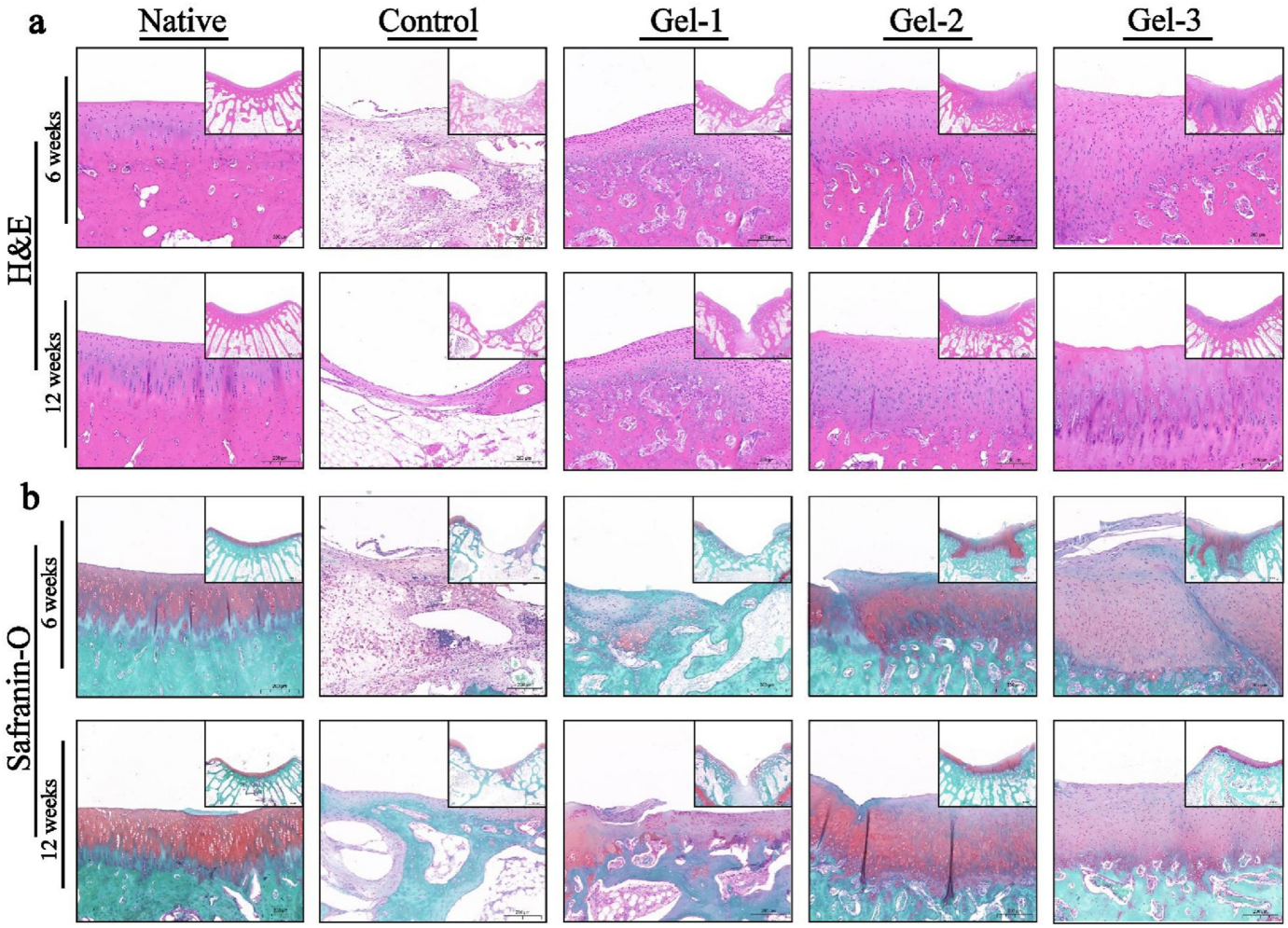

Fig. 8. Histological staining a) H&E and b) Safranin-O staining. (scale = 200 μm).

for 3D culture space for the growth and development of chondrocytes [53]. In addition to the general properties mentioned above, the glycopolypeptide POD hydrogels prepared by the Schiff-base reaction also have high chemical selectivity and rapid performance. Once the Schiff-base bond and gel in the network structure are destroyed, the amino or acylhydrazide groups on the ruptured surface quickly react with the aldehyde groups in contact to reform the Schiff-base bonds, thus reconfiguring the hydrogels matrix for self-repair [54,55]. Therefore, the glycopolypeptide POD hydrogels prepared using the Schiff-base reaction have a dynamic 3D microenvironment that helps to maintain the cell phenotype and promote the ECM deposition.

Glycopolypeptide POD hydrogels can well simulate the microenvironment of chondrocytes. Firstly, the hydrogels own morphology and structure can provide water-rich chondrocytes, accommodate cell growth and development, and allow the cells to contact and communicate with each other in a stable growth environment [56]. Secondly, the pore size of the hydrogels (Gel-1, Gel-2, and Gel-3) provides a space with appropriate mechanical strength for chondrocyte growth and favorable conditions for chondrocyte survival and proliferation in cartilage-tissue engineering [36–38]. In addition, we found that the pore size of the glycopolypeptide POD hydrogels decreased significantly with the increase of Pg concentration, which was attributed to the effect of the higher molecular weight of PLL on the pore size [57,58]. Anti-swelling or low swelling means that the swelling rate of the hydrogels is less than 150% [39,59]. The anti-swelling property can maintain the stability of the mechanical properties and the integrity of the structure of the hydrogels in the water-based environment [60,61]. The positively charged Pg and OD in the glycopolypeptide POD hydrogels show good anti-swelling ability, owing to the mutual attraction of different charges, which provides an important guarantee for the stable mechanical strength of the hydrogels implanted into the body to repair the defect [62–64].

The degradation rate of the glycopolypeptide POD hydrogels well matches the rate of the cartilage-tissue regeneration. The ideal hydrogels network system used in cartilage-tissue regeneration engineering should not only degrade fast enough to allow optimal matrix distribution and tissue, but also slow enough to provide physical support, according to the needs of the regenerated tissue [65]. Unfortunately, even if the cross-linking degree was improved, a sufficiently large number of hydrogels could not reach the degradation rate required for cartilage-tissue repair in a short period of time [66]. Moreover, R. Jin et al. [67] reported that the hydrogels in the PGs analogue based on dextran degraded rapidly. Thus, it can be seen that hydrogels synthesized with PGs face a rapid degradation rate that cannot match the rate of chondrocyte regeneration.

In this study, by degrading three groups of the glycopolypeptide POD hydrogels in PBS and type-II collagenase solutions under physiological conditions, we confirmed the hydrogels' stability and enzyme degradability. The hydrogels hardly degraded in PBS solutions at different time points under physiological conditions. This is because the amide bond in Pg, the OD with the aldehyde group, and the Schiff-base bond formed by the combination of the two are very stable in PBS solutions under

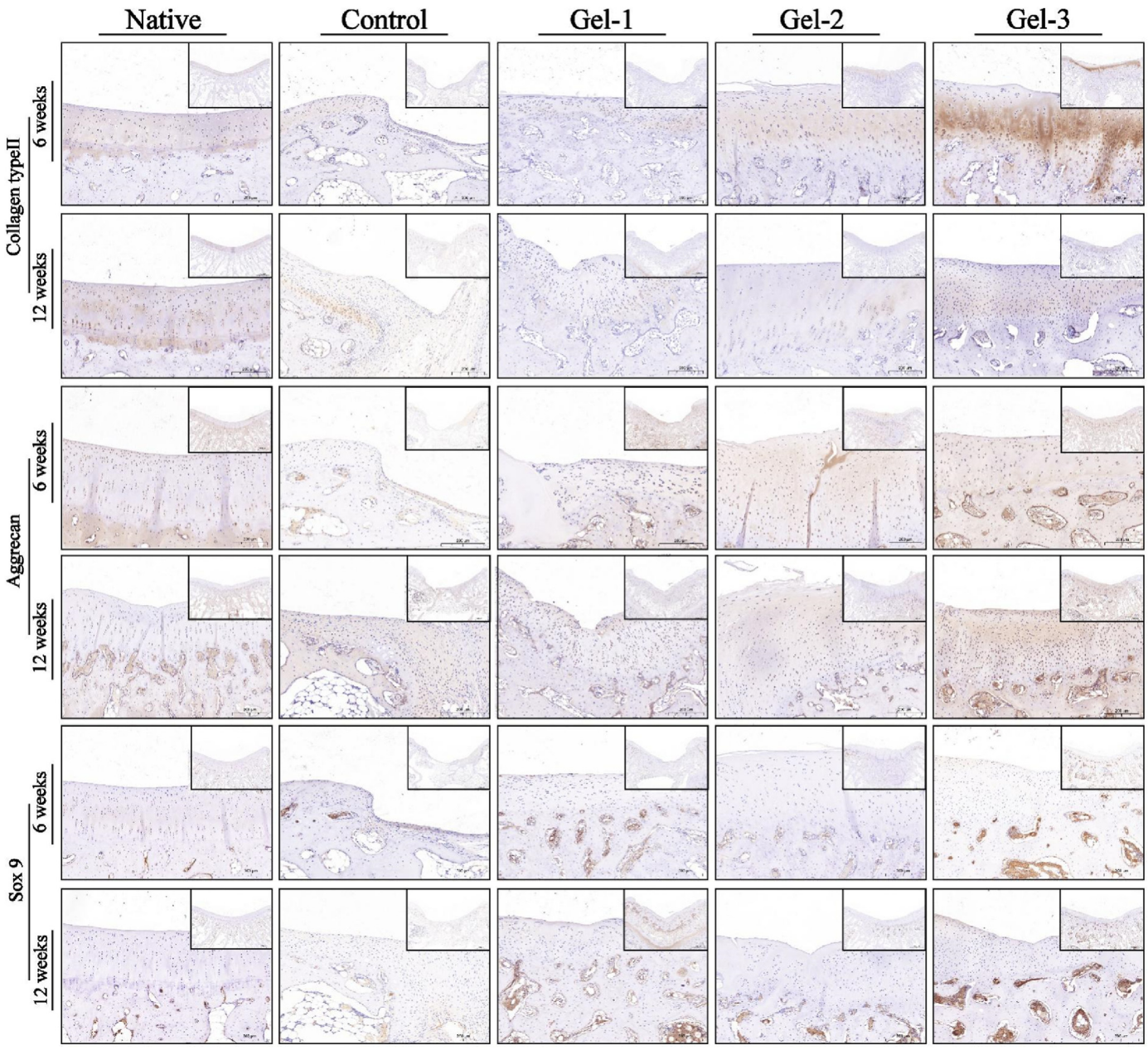

Fig. 9. IHC staining for collagen, aggrecan, and Sox-9. (scale = 200 μm).

physiological conditions [30,68]. However, the glycopolypeptide POD hydrogels degraded significantly in type-II collagenase solutions, which was attributed to the hydrolysis of Schiff-base bond by collagenase [69]. This suggested that it could be degraded by collagenase secreted by the chondrocytes when applied to repair in vivo. In addition, it was suggested that we could adjust the biodegradability of the hydrogels by changing the concentration of the gel components.

Furthermore, increasing the OD concentration improve the cross-linking of hydrogels with Pg and decreases the degradation of the hydrogels [9,10,70]. The adjustable biodegradability of the glycopolypeptide POD hydrogels enables them to match the degradation rate of regenerated tissue. This provides a reference for the reasonable design of polymer-degradation rates in the future. In addition, at 4 weeks, the in vitro enzyme-mediated degradation of Gel-3 was 60 ± 1%, while at 6 weeks, the BMD and BV/TV of the regenerated tissue reached 72% ± 1% of that of natural cartilage tissue, respectively. These results suggest that Gel-3 holds promise for biodegradation to match tissue regeneration. The study still has some limitations, and suggestions for further improvement should be proposed. First, the experimental results of degradation in vitro and regeneration in vivo are a preliminary exploration of the possibility of a dynamic balance between the degradation and regeneration. However, it is still necessary to detect simultaneous degradation and regeneration in animal experiments. Perhaps glycopolypeptide POD hydrogels can be modified by fluorescence for non-invasive detection. Secondly, the self-healing of the glycopolypeptide hydrogels produced by the Schiff-base reaction improved the mechanical properties of the hydrogels system to a certain extent, which improved the stress brittleness of conventional hydrogels. However, the mechanical properties of the hydrogels used in cartilage-tissue regeneration engineering still need to be strengthened. Hence, the glycopolypeptide POD hydrogels should be further modified to introduce polymers or chemical groups that can enhance their mechanical properties.

5. Conclusion

In summary, the glycopolypeptide POD hydrogels were prepared using a simple preparation method. This new PGs analogue had good biocompatibility and adjustable biodegradability matching the tissue regeneration. It was confirmed that glycopolypeptide POD hydrogels promoted the proliferation, adhesion, and migration of chondrocytes, reduced the intracellular ROS of chondrocytes, and alleviated the progress of OA. In addition, it promoted ECM deposition and cartilage-specific gene-expression up-regulation, showing the potential for subchondral bone and hyaline-cartilage formation when repairing cartilage in vivo.

It is worth noting that the Gel-3 group, with a pore size of 122 ± 12 μm, was particularly prominent in the above experiments, and provides a theoretical reference for the design of cartilage-tissue regeneration materials in the future.

Credit author statement

Yinshan Hu and Chengqi Lyu contributed equally to this work. **Yinshan Hu**: Conceptualization, Methodology, Visualization, Investigation, Formal analysis, Writing - original draft. **Chengqi Lyu**: Conceptualization, Investigation, Formal analysis, Writing - Review & Editing. **Lin Teng**: Methodology, Investigation, Formal analysis. **Anqian Wu**: Methodology, Investigation. **Zeyu Zhu**: Methodology, Investigation. **YuShi He**: Methodology, Investigation. **Jiayu Lu**: Writing - Review & Editing, Supervision, Project administration, Funding acquisition.

Declaration of competing interest

The authors declare that they have no known competing financial interests or personal relationships that could have appeared to influence the work reported in this paper.

Data availability

Data will be made available on request.

Acknowledgments

The authors gratefully acknowledge the financial support of the National Natural Science Foundation of China (82071160, 81974152, 82271027), Innovative research team of high-level local universities in Shanghai (Oral and maxillofacial regeneration and functional restoration, SSMU-ZDCX20180900), the Advanced Research Program of Shanghai Jiaotong University Affiliated Sixth People's Hospital (ynlc201810).

Appendix A. Supplementary data

Supplementary data to this article can be found online at https://doi.org/10.1016/j.mtbio.2023.100659.

References

[1] J.N. Katz, K.R. Arant, R.F. Loeser, Diagnosis and treatment of hip and knee osteoarthritis: a review, JAMA, J. Am. Med. Assoc. 325 (2021) 568–578, https://doi.org/10.1001/jama.2020.22171.
[2] E. Sanchez-Lopez, R. Coras, A. Torres, N.E. Lane, M. Guma, Synovial inflammation in osteoarthritis progression, Nat. Rev. Rheumatol. 18 (2022) 258–275, https://doi.org/10.1038/s41584-022-00749-9.
[3] P.R. Coryell, B.O. Diekman, R.F. Loeser, Mechanisms and therapeutic implications of cellular senescence in osteoarthritis, Nat. Rev. Rheumatol. 17 (2021) 47–57, https://doi.org/10.1038/s41584-020-00533-7.
[4] N.K. Arden, T.A. Perry, R.R. Bannuru, O. Bruyère, C. Cooper, I.K. Haugen, M.C. Hochberg, T.E. Mcalindon, A. Mobasheri, J. Reginster, Non-surgical management of knee osteoarthritis: comparison of esceo and oarsi 2019 guidelines, Nat. Rev. Rheumatol. 17 (2021) 59–66, https://doi.org/10.1038/s41584-020-00523-9.
[5] E.A. Makris, A.H. Gomoll, K.N. Malizos, J.C. Hu, K.A. Athanasiou, Repair and tissue engineering techniques for articular cartilage, Nat. Rev. Rheumatol. 11 (2015) 21–34, https://doi.org/10.1038/nrrheum.2014.157.
[6] H. Kwon, W.E. Brown, C.A. Lee, D. Wang, N. Paschos, J.C. Hu, K.A. Athanasiou, Surgical and tissue engineering strategies for articular cartilage and meniscus repair, Nature Reviews, Rheumatology 15 (2019) 550–570, https://doi.org/10.1038/s41584-019-0255-1.
[7] P.G. Conaghan, A.D. Cook, J.A. Hamilton, P.P. Tak, Therapeutic options for targeting inflammatory osteoarthritis pain, Nat. Rev. Rheumatol. 15 (2019) 355–363, https://doi.org/10.1038/s41584-019-0221-y.
[8] X. Ding, H. Zhao, Y. Li, A.L. Lee, Z. Li, M. Fu, C. Li, Y.Y. Yang, P. Yuan, Synthetic peptide hydrogels as 3d scaffolds for tissue engineering, Adv. Drug Deliv. Rev. 160 (2020) 78–104, https://doi.org/10.1016/j.addr.2020.10.005.
[9] O. Jeznach, D. Kołbuk, P. Sajkiewicz, Injectable hydrogels and nanocomposite hydrogels for cartilage regeneration, J. Biomed. Mater. Res., Part A 106 (2018) 2762–2776, https://doi.org/10.1002/jbm.a.36449.
[10] R. Jin, L.S. Moreira Teixeira, A. Krouwels, P.J. Dijkstra, C.A. van Blitterswijk, M. Karperien, J. Feijen, Synthesis and characterization of hyaluronic acid–poly(ethylene glycol) hydrogels via michael addition: an injectable biomaterial for cartilage repair, Acta Biomater. 6 (2010) 1968–1977, https://doi.org/10.1016/j.actbio.2009.12.024.
[11] W. Wei, Y. Ma, X. Yao, W. Zhou, X. Wang, C. Li, J. Lin, Q. He, S. Leptihn, H. Ouyang, Advanced hydrogels for the repair of cartilage defects and regeneration, Bioact. Mater. 6 (2021) 998–1011, https://doi.org/10.1016/j.bioactmat.2020.09.030.
[12] M. Khoshgoftar, P.A. Torzilli, S.A. Maher, Influence of the pericellular and extracellular matrix structural properties on chondrocyte mechanics, J. Orthop. Res. 36 (2018) 721–729.
[13] A.R. Armiento, M.J. Stoddart, M. Alini, D. Eglin, Biomaterials for articular cartilage tissue engineering: learning from biology, Acta Biomater. 65 (2018) 1–20, https://doi.org/10.1016/j.actbio.2017.11.021.
[14] D.J. Huey, J.C. Hu, K.A. Athanasiou, Unlike bone, cartilage regeneration remains elusive, Science 338 (2012) 917–921.
[15] M.R. Servin-Vences, J. Richardson, G.R. Lewin, K. Poole, Mechanoelectrical transduction in chondrocytes, Clin. Exp. Pharmacol. Physiol. 45 (2018) 481–488, https://doi.org/10.1111/1440-1681.12917.
[16] Z. Peng, H. Sun, V. Bunpetch, Y. Koh, Y. Wen, D. Wu, H. Ouyang, The regulation of cartilage extracellular matrix homeostasis in joint cartilage degeneration and regeneration, Biomaterials 268 (2021), 120555, https://doi.org/10.1016/j.biomaterials.2020.120555.
[17] F. Guilak, R.J. Nims, A. Dicks, C. Wu, I. Meulenbelt, Osteoarthritis as a disease of the cartilage pericellular matrix, Matrix Biol. 71–72 (2018) 40–50, https://doi.org/10.1016/j.matbio.2018.05.008.
[18] M. Rahmati, G. Nalesso, A. Mobasheri, M. Mozafari, Aging and osteoarthritis: central role of the extracellular matrix, Ageing Res. Rev. 40 (2017) 20–30, https://doi.org/10.1016/j.arr.2017.07.004.
[19] U. Lindahl, J. Couchman, K. Kimata, J.D. Esko, Proteoglycans and Sulfated Glycosaminoglycans, Cold Spring Harbor Laboratory Press, Cold Spring Harbor (NY), 2015.
[20] W. Lin, J. Klein, Recent progress in cartilage lubrication, Adv. Mater. 33 (2021), 2005513, https://doi.org/10.1002/adma.202005513.
[21] C. Kiani, L. Chen, Y.J. Wu, A.J. Yee, B.B. Yang, Structure and function of aggrecan, Cell Res. 12 (2002) 19–32, https://doi.org/10.1038/sj.cr.7290106.
[22] A.J. Hayes, J. Melrose, Glycosaminoglycan and proteoglycan biotherapeutics in articular cartilage protection and repair strategies: novel approaches to visco-supplementation in orthobiologics, Adv. Ther. 2 (2019), 1900034, https://doi.org/10.1002/adtp.201900034.
[23] P. Zarrintaj, S. Ghorbani, M. Barani, N.P. Singh Chauhan, M. Khodadadi Yazdi, M.R. Saeb, J.D. Ramsey, M.R. Hamblin, M. Mozafari, E. Mostafavi, Polylysine for skin regeneration: a review of recent advances and future perspectives, Bioeng. Transl. Med. 7 (2022), e10261, https://doi.org/10.1002/btm2.10261.
[24] J.D. San Antonio, R.S. Tuan, Chondrogenesis of limb bud mesenchyme in vitro: stimulation by cations, Dev. Biol. 115 (1986) 313–324, https://doi.org/10.1016/0012-1606(86)90252-6.
[25] J. Lam, E.C. Clark, E.L.S. Fong, E.J. Lee, S. Lu, Y. Tabata, A.G. Mikos, Evaluation of cell-laden polyelectrolyte hydrogels incorporating poly(l-lysine) for applications in cartilage tissue engineering, Biomaterials 83 (2016) 332–346, https://doi.org/10.1016/j.biomaterials.2016.01.020.
[26] Z. Zhou, W. Wu, J. Fang, J. Yin, Polymer-based porous microcarriers as cell delivery systems for applications in bone and cartilage tissue engineering, Int. Mater. Rev. 66 (2021) 77–113.
[27] D. Pranantyo, L.Q. Xu, Z. Hou, E. Kang, M.B. Chan-Park, Increasing bacterial affinity and cytocompatibility with four-arm star glycopolymers and antimicrobial α-polylysine11electronic supplementary information (esi) available: supplementary synthesis procedures and characterization figures, Polym. Chem. 8 (2017) 3364–3373, https://doi.org/10.1039/c7py00441a. See doi: 10.1039/c7py00441a.
[28] Z. Li, B. Li, X. Li, Z. Lin, L. Chen, H. Chen, Y. Jin, T. Zhang, H. Xia, Y. Lu, Y. Zhang, Ultrafast in-situ forming halloysite nanotube-doped chitosan/oxidized dextran hydrogels for hemostasis and wound repair, Carbohydr. Polym. 267 (2021), 118155, https://doi.org/10.1016/j.carbpol.2021.118155.
[29] L. Fan, C. Lin, P. Zhao, X. Wen, G. Li, An injectable bioorthogonal dextran hydrogel for enhanced chondrogenesis of primary stem cells, Tissue Eng. C Methods 24 (2018) 504–513, https://doi.org/10.1089/ten.tec.2018.0085.
[30] K. Matsumura, N. Nakajima, H. Sugai, S. Hyon, Self-degradation of tissue adhesive based on oxidized dextran and poly-l-lysine, Carbohydr. Polym. 113 (2014) 32–38, https://doi.org/10.1016/j.carbpol.2014.06.073.

[31] L. Teng, Z. Shao, Q. Bai, X. Zhang, Y.S. He, J. Lu, D. Zou, C. Feng, C.M. Dong, Biomimetic glycopolypeptide hydrogels with tunable adhesion and microporous structure for fast hemostasis and highly efficient wound healing, Adv. Funct. Mater. 31 (2021), 2105628.
[32] X. Wei, W. Zhou, Z. Tang, H. Wu, Y. Liu, H. Dong, N. Wang, H. Huang, S. Bao, L. Shi, X. Li, Y. Zheng, Z. Guo, Magnesium surface-activated 3d printed porous peek scaffolds for in vivo osseointegration by promoting angiogenesis and osteogenesis, Bioact. Mater. 20 (2023) 16–28, https://doi.org/10.1016/j.bioactmat.2022.05.011.
[33] Y. Sun, Y. You, W. Jiang, Z. Zhai, K. Dai, 3d-bioprinting a genetically inspired cartilage scaffold with gdf5-conjugated bmsc-laden hydrogel and polymer for cartilage repair, Theranostics 9 (2019) 6949–6961, https://doi.org/10.7150/thno.38061.
[34] L. Teng, Z. Shao, Q. Bai, X. Zhang, Y. He, J. Lu, D. Zou, C. Feng, C. Dong, Biomimetic glycopolypeptide hydrogels with tunable adhesion and microporous structure for fast hemostasis and highly efficient wound healing, Adv. Funct. Mater. 31 (2021), 2105628, https://doi.org/10.1002/adfm.202105628.
[35] P. Yadav, G. Beniwal, K.K. Saxena, A review on pore and porosity in tissue engineering, Mater. Today: Proc. 44 (2021) 2623–2628, https://doi.org/10.1016/j.matpr.2020.12.661.
[36] Z. Abpeikar, P.B. Milan, L. Moradi, M. Anjomshoa, S. Asadpour, Influence of pore sizes in 3d-scaffolds on mechanical properties of scaffolds and survival, distribution, and proliferation of human chondrocytes, Mech. Adv. Mater. Struct. (2021) 1–12, https://doi.org/10.1080/15376494.2021.1943077.
[37] W. Bao, M. Li, Y. Yang, Y. Wan, X. Wang, N. Bi, C. Li, Advancements and frontiers in the high performance of natural hydrogels for cartilage tissue engineering, Front. Chem. 8 (2020).
[38] H.D.N. Tran, K.D. Park, Y.C. Ching, C. Huynh, D.H. Nguyen, A comprehensive review on polymeric hydrogel and its composite: matrices of choice for bone and cartilage tissue engineering, J. Ind. Eng. Chem. 89 (2020) 58–82, https://doi.org/10.1016/j.jiec.2020.06.017.
[39] Y. Zhan, W. Fu, Y. Xing, X. Ma, C. Chen, Advances in versatile anti-swelling polymer hydrogels, Mater. Sci. Eng. C 127 (2021), 112208, https://doi.org/10.1016/j.msec.2021.112208.
[40] P.X. Ma, Biomimetic materials for tissue engineering, Adv. Drug Deliv. Rev. 60 (2008) 184–198, https://doi.org/10.1016/j.addr.2007.08.041.
[41] L. Wang, K. Yang, X. Li, X. Zhang, D. Zhang, L. Wang, C. Lee, A double-crosslinked self-healing antibacterial hydrogel with enhanced mechanical performance for wound treatment, Acta Biomater. 124 (2021) 139–152, https://doi.org/10.1016/j.actbio.2021.01.038.
[42] F.J. Blanco, I. Rego, C. Ruiz-Romero, The role of mitochondria in osteoarthritis, Nat. Rev. Rheumatol. 7 (2011) 161–169, https://doi.org/10.1038/nrrheum.2010.213.
[43] X. Zhang, Z. Li, P. Yang, G. Duan, X. Liu, Z. Gu, Y. Li, Polyphenol scaffolds in tissue engineering, Mater. Horiz. 8 (2021) 145–167, https://doi.org/10.1039/D0MH01317J.
[44] F. Qu, F. Guilak, R.L. Mauck, Cell migration: implications for repair and regeneration in joint disease, Nat. Rev. Rheumatol. 15 (2019) 167–179, https://doi.org/10.1038/s41584-018-0151-0.
[45] M. Arra, G. Swarnkar, K. Ke, J.E. Otero, J. Ying, X. Duan, T. Maruyama, M.F. Rai, R.J. O Keefe, G. Mbalaviele, J. Shen, Y. Abu-Amer, Ldha-mediated ros generation in chondrocytes is a potential therapeutic target for osteoarthritis, Nat. Commun. 11 (2020) 3427, https://doi.org/10.1038/s41467-020-17242-0.
[46] W. Qi, W. Yuan, J. Yan, H. Wang, Growth and accelerated differentiation of mesenchymal stem cells on graphene oxide/poly-l-lysine composite films, J. Mater. Chem. B 2 (2014) 5461–5467, https://doi.org/10.1039/C4TB00856A.
[47] J. Lam, E.C. Clark, E.L.S. Fong, E.J. Lee, S. Lu, Y. Tabata, A.G. Mikos, Evaluation of cell-laden polyelectrolyte hydrogels incorporating poly(l-lysine) for applications in cartilage tissue engineering, Biomaterials 83 (2016) 332–346, https://doi.org/10.1016/j.biomaterials.2016.01.020.
[48] L. Bian, M. Guvendiren, R.L. Mauck, J.A. Burdick, Hydrogels that mimic developmentally relevant matrix and n-cadherin interactions enhance msc chondrogenesis, Proc. Natl. Acad. Sci. U.S.A. 110 (2013) 10117–10122, https://doi.org/10.1073/pnas.1214100110.
[49] B. Zimmermann, Assembly and disassembly of gap junctions during mesenchymal cell condensation and early chondrogenesis in limb buds of mouse embryos, J. Anat. 138 (1984) 351–363.
[50] V. Graceffa, C. Vinatier, J. Guicheux, M. Stoddart, M. Alini, D.I. Zeugolis, Chasing chimeras – the elusive stable chondrogenic phenotype, Biomaterials 192 (2019) 199–225, https://doi.org/10.1016/j.biomaterials.2018.11.014.
[51] V. Graceffa, C. Vinatier, J. Guicheux, C.H. Evans, M. Stoddart, M. Alini, D.I. Zeugolis, State of art and limitations in genetic engineering to induce stable chondrogenic phenotype, Biotechnol. Adv. 36 (2018) 1855–1869, https://doi.org/10.1016/j.biotechadv.2018.07.004.
[52] U. Freudenberg, Y. Liang, K.L. Kiick, C. Werner, Glycosaminoglycan-based biohybrid hydrogels: a sweet and smart choice for multifunctional biomaterials, Adv. Mater. 28 (2016) 8861–8891, https://doi.org/10.1002/adma.201601908.
[53] S.C. Neves, L. Moroni, C.C. Barrias, P.L. Granja, Leveling up hydrogels: hybrid systems in tissue engineering, Trends Biotechnol. 38 (2020) 292–315, https://doi.org/10.1016/j.tibtech.2019.09.004.
[54] C. Mo, L. Xiang, Y. Chen, Advances in injectable and self-healing polysaccharide hydrogel based on the schiff base reaction, Macromol. Rapid Commun. 42 (2021), 2100025, https://doi.org/10.1002/marc.202100025.
[55] Y. Jia, J. Li, Molecular assembly of schiff base interactions: construction and application, Chem. Rev. 115 (2015) 1597–1621, https://doi.org/10.1021/cr400559g.
[56] M. Cucchiarini, H. Madry, Biomaterial-guided delivery of gene vectors for targeted articular cartilage repair, Nat. Rev. Rheumatol. 15 (2019) 18–29, https://doi.org/10.1038/s41584-018-0125-2.
[57] J.J. Schmidt, J. Rowley, H.J. Kong, Hydrogels used for cell-based drug delivery, J. Biomed. Mater. Res., Part A 87A (2008) 1113–1122, https://doi.org/10.1002/jbm.a.32287.
[58] F. Hajifathaliha, A. Mahboubi, N. Bolourchian, E. Mohit, L. Nematollahi, Multilayer alginate microcapsules for live cell microencapsulation; Is there any preference for selecting cationic polymers? Iran. J. Pharm. Res. (IJPR): Ijpr 20 (2021) 173.
[59] Y.S. Zhang, A. Khademhosseini, Advances in engineering hydrogels, Science 356 (2017) eaaf3627, https://doi.org/10.1126/science.aaf3627.
[60] S. Wang, J. Liu, L. Wang, H. Cai, Q. Wang, W. Wang, J. Shao, X. Dong, Underwater adhesion and anti-swelling hydrogels, Adv. Mater. Technol. n/a (2022), 2201477, https://doi.org/10.1002/admt.202201477.
[61] J. Hua, P.F. Ng, B. Fei, High-strength hydrogels: microstructure design, characterization and applications, J. Polym. Sci. B Polym. Phys. 56 (2018) 1325–1335, https://doi.org/10.1002/polb.24725.
[62] H. Zhang, J. He, J. Qu, High-strength, tough, and anti-swelling schiff base hydrogels with fluorescent encryption writing, solvent response and double shape memory functions, Eur. Polym. J. 178 (2022), 111487.
[63] Y. Ou, M. Tian, Advances in multifunctional chitosan-based self-healing hydrogels for biomedical applications, J. Mater. Chem. B 9 (2021) 7955–7971.
[64] W. Qiu, Q. Wang, M. Li, N. Li, X. Wang, J. Yu, F. Li, D. Wu, 3d hybrid scaffold with aligned nanofiber yarns embedded in injectable hydrogels for monitoring and repairing chronic wounds, Compos. B Eng. 234 (2022), 109688.
[65] I.L. Kim, R.L. Mauck, J.A. Burdick, Hydrogel design for cartilage tissue engineering: a case study with hyaluronic acid, Biomaterials 32 (2011) 8771–8782, https://doi.org/10.1016/j.biomaterials.2011.08.073.
[66] E. öztürk, Ø. Arlov, S. Aksel, L. Li, D.M. Ornitz, G. Skjåk-Bræk, M. Zenobi-Wong, Sulfated hydrogel matrices direct mitogenicity and maintenance of chondrocyte phenotype through activation of fgf signaling, Adv. Funct. Mater. 26 (2016) 3649–3662, https://doi.org/10.1002/adfm.201600092.
[67] R. Jin, L.S. Moreira Teixeira, P.J. Dijkstra, C.A. van Blitterswijk, M. Karperien, J. Feijen, Enzymatically-crosslinked injectable hydrogels based on biomimetic dextran–hyaluronic acid conjugates for cartilage tissue engineering, Biomaterials 31 (2010) 3103–3113, https://doi.org/10.1016/j.biomaterials.2010.01.013.
[68] Y. Jia, X. Yan, J. Li, Schiff base mediated dipeptide assembly toward nanoarchitectonics, Angew. Chem. Int. Ed. 61 (2022), e202207752, https://doi.org/10.1002/anie.202207752.
[69] P. Li, Y. Zhong, X. Wang, J. Hao, Enzyme-regulated healable polymeric hydrogels, Acs Central Sci 6 (2020) 1507–1522, https://doi.org/10.1021/acscentsci.0c00768.
[70] X. Zhang, Y. Jiang, L. Han, X. Lu, Biodegradable polymer hydrogel-based tissue adhesives: a review, Biosurface and Biotribology 7 (2021) 163–179, https://doi.org/10.1049/bsb2.12016.